Abelian and non-Abelian anyons in integer quantum anomalous Hall effect and topological phase transitions via superconducting proximity effect

Xuele Liu, Ziqiang Wang, X. C. Xie, and Yue Yu

Phys. Rev. B **83**, 125105 — Published 18 March 2011

DOI: 10.1103/PhysRevB.83.125105

Abelian and non-abelian anyons in integer quantum anomalous Hall effect and topological phase transitions via superconducting proximity effect

Xuele Liu,[1,2] Ziqiang Wang,[3] X.C. Xie,[4,2] and Yue Yu[1,*]

[1] *Institute of Theoretical Physics, Chinese Academy of Sciences, P.O. Box 2735, Beijing 100190, China*
[2] *Department of Physics, Oklahoma State University, Stillwater, Oklahoma 74078, USA*
[3] *Department of Physics, Boston College, Chestnut Hill, MA 02467, USA*
[4] *International Center for Quantum Materials, Peking University, Beijing 100871, China*

(Dated: February 4, 2011)

We study the quantum anomalous Hall effect described by a class of two-component Haldane models on square lattices. We show that the latter can be transformed into a pseudospin triplet $p + ip$-wave paired superfluid. In the long wave length limit, the ground state wave function is described by Halperin's $(1, 1, -1)$ state of neutral fermions analogous to the double layer quantum Hall effect. The vortex excitations are charge $e/2$ *abelian anyons* which carry a neutral Dirac fermion zero mode. The superconducting proximity effect induces 'tunneling' between 'layers' which leads to topological phase transitions whereby the Dirac fermion zero mode fractionalizes and Majorana fermions emerge in the edge states. The charge $e/2$ vortex excitation carrying a Majorana zero mode is a non-abelian anyon. The proximity effect can also drive a conventional insulator into a quantum anomalous Hall effect state with a Majorana edge mode and the non-abelian vortex excitations.

PACS numbers: 71.10.Pm, 74.45.+c, 03.67.Lx, 74.90.+n

I. INTRODUCTION

The discovery of the quantum Hall effect (QHE)[1] opened an era for studying topological quantum phases[2]. Some twenty years ago, Haldane[3] proposed the quantum anomalous Hall effect (QAHE) for electrons on a two-dimensional lattice. This is generalized to the time reversal invariant topological insulators[4] in two dimensions[5–8] and three dimensions[9–13]. With the band inversion in these system, it raises the hope for realizing the QAHE in a two-band model of two-dimensional magnetic insulators[14]. Candidate materials for this effect, HgTe doped with Mn[15] and a tetradymite semiconductors doped with transition metal elements[16], have been predicted. Other proposals are also made in condensed matter systems recently[17,18]. The QAHE has also been proposed for cold atom systems[19–21].

Another advance is the search for topological phases with non-abelian anyons[22] that have potential applications for quantum computing[23]. In addition to the $\nu = 5/2$ fractional QHE, it has been shown theoretically that the superconducting proximity effect on the surface state of topological insulator[24] and on semiconductors with strong spin-orbit coupling and Zeeman splitting[25] provides a new avenue for generating the Majorana zero mode and non-abelian vortex excitations.

In this work, we study the QAHE for a class of two-component Haldane models on a square lattice. The physical degrees of freedom represented by the components depend on the microscopic details: the real spins of electrons, band indices[14], the top-bottom surface states of three-dimensional topological insulator[16], as well as the sublattice indices as exemplified below. We show that, in a pseudospin representation, the QAHE system can be transformed into a chiral $p + ip$-wave pairing state involving both pseudospin components. The ground state wave function is given by a determinant of the pairing functions whose long wave length limit is a charge neutral Halperin $(1, 1, -1)$ state analogous to the double layer QHE[26]. There are abelian anyon excitations with charge $e/2$, despite that the present model describes an *integer* QAHE system.

When s-wave superconductor develops in the QAHE system due to the proximity effect, tunneling between the different isospin components takes place. We find that the system displays continuous transitions between topological phases with abelian and non-abelian anyon excitations. Specifically, a topological phase transition from the Hall conductance $2e^2/h$ to e^2/h happens for sufficiently strong proximity induced pairing because one of the pseudospin components is driven to a strong pairing state analogous to that in the $\nu = 1/2$ double-layer fractional QHE discussed by Ho[27] and Read and Green[28]. The remaining pseudospin component is in the weak pairing state described by a Moore-Read Pfaffian[22]. A Majorana zero mode appears in the edge state and the vortex excitation carrying this Majorana mode is a non-abelian anyon. Interestingly, the model also exhibits a topological trivial phase without the QAHE when the triplet $p + ip$-wave pairing is in a *topologically unprotected* weak pairing state. We find that the proximity effect can drive one of the pseudospin components into a topologically protected weak pairing state with quantized Hall conductance $-e^2/h$, edge Majorana zero mode, and non-abelian anyon vortex excitations (see also Ref.[29]).

This paper was organized as follows:

II. MODELS

The Hamiltonian of the two-component model in the lattice momentum space is given by

$$\begin{aligned} H_0 &= \sum_{\mathbf{k}}[(p_x+ip_y)c^\dagger_{a\mathbf{k}}c_{b\mathbf{k}}+h.c. \\ &+ h_z(\mathbf{k})(c^\dagger_{a\mathbf{k}}c_{a\mathbf{k}}-c^\dagger_{b\mathbf{k}}c_{b\mathbf{k}})+h_0(\mathbf{k})(c^\dagger_{a\mathbf{k}}c_{a\mathbf{k}}+c^\dagger_{b\mathbf{k}}c_{b\mathbf{k}})] \end{aligned} \quad (1)$$

where $c_{a(b)\mathbf{k}}$ annihilate an electron of component $a(b)$ with momentum $\mathbf{k}$ and $h_0(\mathbf{k})$ is the dispersion due to hopping among electrons of the same component. The physical origin of the terms proportional to p_x+ip_y and h_z depends on the system of interest. If (a,b) label the electron spin, $p_x+ip_y\to k_x+ik_y$ arises from Rashba spin-orbit coupling[14] and h_z is the magnetization. If (a,b) are the orbital indices, p_x+ip_y describes the orbital hybridyzation[14,15] and h_z is the crystal field splitting. For the doped tetradymite semiconductors, they constitute the spin-orbit coupling associated with the three-dimensional topological insulator[16].

A. A Generalized Haldane Model in Square Lattice

In Fig. 1, we give an explicit realization of the Hamiltonian (1) for spinless fermions on a square lattice where (a,b) label the A and B sublattices. This turns out to be a modified Haldane's model where the complex hopping induces $\pm\pi$ staggered plaquette flux with the link phase distribution shown in Fig.1 (right panel). The corresponding Halimtonian with this setup is given by

$$\begin{aligned} H_0 &= -t\sum_{i_a}[c^\dagger_{i_a+\delta_x}c_{i_a}+ic^\dagger_{i_a+\delta_y}c_{i_a}+h.c.] \\ &+ t\sum_{i_b}[c^\dagger_{i_b+\delta_x}c_{i_b}-ic^\dagger_{i_b+\delta_y}c_{i_b}+h.c.] \\ &- t'\sum_{i_a}[c^\dagger_{i_a+\delta_{aa1}}c_{i_a}+c^\dagger_{i_a+\delta_{aa2}}c_{i_a}+h.c.] \\ &+ t'\sum_{i_b}[c^\dagger_{i_b+\delta_{bb1}}c_{i_b}+c^\dagger_{i_b+\delta_{bb2}}c_{i_b}+h.c.] \\ &- M\sum_i(c^\dagger_{i_a}c_{i_a}-c^\dagger_{i_b}c_{i_b}) \end{aligned} \quad (2)$$

where $c^\dagger_{i_{a,b}}$ is the creation operator of the electron at the site $i_{a,b}$ on the A or B sublattice. The coordinates and vectors are figured in the left panel of Fig. 1. The lattice spacing a is set to be unit. t and t' are the nearest neighbor hopping amplitude and the next nearest neighbor's. $\pm M$ is the on-site energy on i_a and i_b, respectively. It can also be realized in cold atom context with a simpler staggered flux while the atom orbital is different on the A and B sublattice[20].

Making the Fourier transformation, the Hamiltonian is exactly given by Eq. (1) with $p_x+ip_y=-2t(\sin k_y+i\sin k_x)$, $h_z(\mathbf{k})=-M-4t'\cos k_x\cos k_y$, and $h_0=0$, where t and t' are the hopping amplitudes between nearest and next nearest neighbors indicated in Fig.1 and $\pm M$ is the on-site energy for the A and B sublattices. Note that the 'magnetization' contains $\cos k_x\cos k_y$ and is different from that used in[14]. A similar model can also be realized in cold atom systems[20]. For $h_0=0$, there is an important $O(2)$ symmetry associated with the $U(1)$ particle number conservation and a $\mathbb{Z}_2$ under $c^\dagger_{a,\mathbf{k}}\to ic_{b,-\mathbf{k}}$, i.e., a $\mathcal{C}\cdot\mathcal{S}$ (particle-hole $\cdot$ sublattice) symmetry. If $h_0\neq 0$ but can be adiabatically driven to zero, we think the results of this work are also valid.

We now study Hamiltonian (1) in the A-B sublattice where $\mathbf{k}$ is confined to the *reduced* first Brillouin zone bounded by $k_x\pm k_y=\pm\pi$ due to the A-B sublattices. Our results can be extended directly to other relevant cases discussed above with lattice translation symmetry.

The eigen-energy of (1) is given by $E_0=\pm\sqrt{h_z^2+|p|^2}$. There are two independent Dirac points at $(0,0)$ and $(\pi,0)$ in the reduced zone. When an extended s-wave pairing is induced by proximity effect[24] on the QAHE system, the total Hamiltonian is given by $H=H_0+H_{sc}$, where

$$H_{sc}=\sum_{\mathbf{k}}f(\mathbf{k})(c_{a-\mathbf{k}}c_{b\mathbf{k}}+c^\dagger_{b\mathbf{k}}c^\dagger_{a-\mathbf{k}}), \quad (3)$$

and $f(\mathbf{k})=2\Delta(\cos k_x+\cos k_y)$. The eigen-energy of the total Hamiltonian is given by $E=\pm\sqrt{(h_z\pm f)^2+|p|^2}$. The energy gap of the QAHE at the Dirac point $(0,0)$ closes when $\Delta=\frac{1}{4}(M+4t')$, whereas the QAHE gap at $(\pi,0)$ is unperturbed since $f(\mathbf{k})=0$ for $k_x\pm k_y=\pm\pi$.

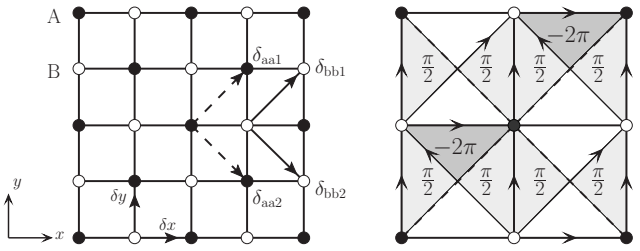

FIG. 1: The square lattice model for Hamiltonian (1) Left: The two-sublattice and hopping. Right: The flux distribution. Hopping along arrowed vertical links generates a phase π and arrowed horizontal links a phase $\pi/2$. A net flux of -2π ($\pi/2$) is accumulated for the dark (light) grey *triangular blocks*. The rest of the hopping is real.

To unveil the ground state wavefunction and the topological properties of Eq. (1), we introduce a pseudospin representation by mixing the electron and hole of different component (which in fact indicates a particle-hole transformation of b-component)

$$c_{\uparrow\mathbf{k}}=(c_{a\mathbf{k}}+c^\dagger_{b-\mathbf{k}})/\sqrt{2},\quad c_{\downarrow\mathbf{k}}=i(c_{a\mathbf{k}}-c^\dagger_{b-\mathbf{k}})/\sqrt{2}. \quad (4)$$

Under this unitary transformation, the Hamiltonian in

terms of fermions carrying the pseudospin becomes

$$H_0 = \sum_{\mathbf{k};s=\uparrow,\downarrow} [h_z c^\dagger_{s\mathbf{k}} c_{s\mathbf{k}} - ((p_x - ip_y)c_{s\mathbf{k}}c_{s-\mathbf{k}} + h.c.)/2]. \quad (5)$$

Both the pseudospin-$\uparrow$ and $\downarrow$ fermions, having a band dispersion $h_z(\mathbf{k})$, are in the $p+ip$-wave paired states. Hamiltonian (5) is closely related to the $\nu = 1/2$ double-layer fractional QHE if we identify the pseudospins with the even/odd states of the isospin (layer index) in the context of triplet chiral p-wave pairing[27,28].

B. Winding Numbers

We now calculate the winding number, which describes the mapping from the reduced zone (a torus) to a target sphere specified by the unit vector $\mathbf{n} = \frac{(p_x, p_y, h_z)}{E_0}$. The winding number is given by $C = C_\uparrow + C_\downarrow$ with $C_s = \frac{1}{4\pi}\int d^2k \mathbf{n}\cdot\partial_{k_x}\mathbf{n}\times\partial_{k_y}\mathbf{n}$ in the continuum limit. A direct calculation yields $C_\uparrow = C_\downarrow = 1$ and $C = 2$ which reflects the fact that the whole first Brillouin zone covers twice of the sphere with such a map $\mathbf{n}$. This result can be understood intuitively by considering the vector components of $\mathbf{n}$ near the two Dirac points $(0,0)$ and $(\pi,0)$. For a small deviation $\mathbf{q} \sim 0$, they are $(-2tq_y, 2tq_x, -M-4t')/E_0$ near $(0,0)$ and $(-2tq_y, -2q_x, -M+4t')/E_0$ near $(\pi,0)$ (See Fig. 2). Therefore, the Dirac points are mapped to the north and south poles which are covered once. A semi-sphere including a pole contributes $\pm 1/2$ to the winding number depending on the pole's frame. When $M < 4t'$, both poles are in the right hand frame and each semi-sphere contributes $1/2$ which gives $C_{\uparrow,\downarrow} = 1$ and $C = 2$. Thus, this QAHE has Hall conductance $2\frac{e^2}{h}$.

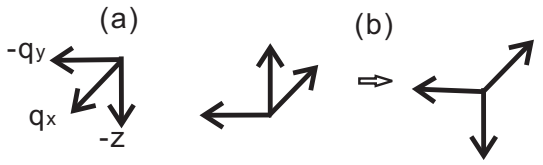

FIG. 2: : The frames and frame change from $M < 4t'$ to $M > 4t'$. (a) $(-2tq_y, 2tq_x, -M-4t')$ at $(0,0)$. The frame is not changed and is the right. (b) $(-2tq_y, -2q_x, -M+4t')$ at $(\pi,0)$. The frame is changed from the right for $M < 4t'$ to the left for $M > 4t'$.

III. GROUND STATES AND ANYONIC EXCITATIONS

A. The (1,1,-1)-state and abelian anyons

The paired state has BCS coherence factors $|u_{s,\mathbf{k}}|^2 = \frac{1}{2}(1+\frac{h_z}{E_0}), |v_{s,\mathbf{k}}|^2 = \frac{1}{2}(1-\frac{h_z}{E_0})$ and pairing functions

$$g_s(\mathbf{k}) = v_{s,\mathbf{k}}/u_{s,\mathbf{k}} = g(\mathbf{k}) = -(E_0 - h_z)/p. \quad (6)$$

For $M < 4t'$, the effective chemical potential at the Dirac point $(\pi,0)$ $\mu_{(\pi,0)} = -h_{z,(\pi,0)} = M - 4t' < 0$ such that $u_s \sim 1$ and $g_s \sim v_s \sim q_y + iq_x$. This is in the strong pairing regime[28] and can be thought as the 'infinity' point in the continuum theory. On the other hand, the effective chemical potential at the Dirac point $(0,0)$ $\mu_{(0,0)} = -h_{z;(0,0)} = M + 4t' > 0$ which leads to $v_s \sim 1$ and $g_s \sim 1/u_s \sim 1/(q_y - iq_x)$. This singular pairing function in the long wavelength limit is the hallmark of the topologically nontrivial $p+ip$ weak pairing phase[28]. Therefore, the long distance, low energy physics is determined by the weak pairing of the qusiparticles carrying both pseudospins near the Dirac point $(0,0)$. The ground state is given by

$$|G_s\rangle \propto \exp[\frac{1}{2}\sum_{\mathbf{k}} g(\mathbf{k})(c^\dagger_{\uparrow\mathbf{k}}c^\dagger_{\uparrow-\mathbf{k}} + c^\dagger_{\downarrow\mathbf{k}}c^\dagger_{\downarrow-\mathbf{k}})]|0_s\rangle, \quad (7)$$

where $|0_s\rangle$ is the vacuum for the fermions carrying the pseudospin, $c_{s\mathbf{k}}|0_s\rangle = 0$. From the transformation (4), it is clear that this vacuum is empty of the a-electrons but filled with the b-electrons. The ground state in Eq. (7) resembles the neutral part of the $(3,3,1)$-state in $\nu = 1/2$ double layer fractional QHE[26,28]. Going back to the original a-b component electrons, the ground state wave function of Eq. (1) is of the form of a *determinant of the pairing function* $g(\mathbf{r})$, the Fourier image of $g(\mathbf{k})$,

$$\Psi(\{\mathbf{r}^a_i, \mathbf{r}^b_i\}) = \langle 0|\prod_i c_a(\mathbf{r}^a_i)c_b(\mathbf{r}^b_i)|G\rangle \propto \det[g(\mathbf{r}^a_i - \mathbf{r}^b_j)],$$

where $\mathbf{r}^{a,b}_i$ are the coordinates of the two-component electrons in the ground state $|G\rangle$ out of the vacuum $c_{a(b)k}|0\rangle = 0$. The ground state $|G\rangle$ and the vacuum $|0\rangle$ of the original Hamiltonian (1) are related to $|G_s\rangle$ and $|0_s\rangle$ in the pseudospin representation by $|G_s\rangle = U|G\rangle$, $|0_s\rangle = U|0\rangle$ where U is the unitary operator for the particle-hole transformation in the b-component indicated in Eq. (4). In the long wavelength limit, the weak pairing near $(0,0)$ implies $g(\mathbf{r}^a_i - \mathbf{r}^b_j) \sim \frac{1}{z^a_i - z^b_j}$. Using Cauchy's determinant identity, we find

$$\Psi(\{\mathbf{r}^a_i, \mathbf{r}^b_i\}) \sim \prod_{i<j}(z^a_i - z^a_j)\prod_{k<l}(z^b_k - z^b_l)\prod_{sr}(z^a_s - z^b_r)^{-1}.$$

This is exactly the charge neutral part of the (3,3,1), i.e. a $(1,1,-1)$-state.

The above result allows us to describe localized charge excitations in the filled bands which are carried by the finite $\mathbf{k}$ states. A Laughlin-type quasihole excitation is a good approximation of a real hole with charge e because the number of extended states in the QAHE system is the same as that in a band insulator. Thus, the minimal charge $e/2$ vortex pair excitations located at η_1 and η_2 are similar to that in the (3,3,1) state, i.e.,

$$\Psi_v(\eta_1, \eta_2) \sim \det\{[(z^a_i - \eta_1)(z^b_j - \eta_2) + (1 \leftrightarrow 2)]g(\mathbf{r}^a_i - \mathbf{r}^b_j)\}.$$

We thus come to the conclusion that the vortex excitations in this integer QAHE system are charge $e/2$ abelian

anyons carrying a neutral Dirac fermion zero mode. This fractional charge can also be understood from the ground state degeneracy. In Eq. (5), the $O(2)$ symmetry is generated by the pseudospin $S_y = -i\sum_{\mathbf{k}}(c^\dagger_{\uparrow\mathbf{k}}c_{\downarrow\mathbf{k}} - c^\dagger_{\downarrow\mathbf{k}}c_{\uparrow\mathbf{k}})/2$ and $c_{\uparrow\mathbf{k}} \leftrightarrow c_{\downarrow\mathbf{k}}$. Thus, the ground state is four-fold degenerate and the vortex excitations carry $S_y = 1/4$[28]. In terms of the original QAHE system, $2S_y$ corresponds to the charge operator $N_a + N_b$ due to the partial particle-hole transformation. Thus, the vortex carries charge $e/2$, which is different from $e/4$ in the (3,3,1)-state. The vortex pairs have an excitation energy on the order of $e^2/(4|\eta_1 - \eta_2|)$ and are thus stable when the vortices are well separated by the distance $l > e^2/[8(M+4t')]$. When the vortices are close enough so that their energy is higher than the band gap, they fuse into a real hole.

B. Weak-strong pairing phase transition and non-abelian anyons

In the pseudospin representation, the pairing due to the proximity effect in Eq. (3) plays the role of a magnetic field and h_z in Eq. (5) splits into $h_{z;\uparrow,\downarrow} = h_z \mp f(\mathbf{k})$ for $c_{\uparrow,\downarrow}$, respectively. In the double-layer language, this $f(\mathbf{k})$ amounts to interlayer tunneling that splits the symmetric and antisymmetric combinations. The antisymmetric component can be driven into a strong pairing state, leaving only the symmetric one governing the physics at low energy and long wavelength[27]. The winding number associated with the pseudospin-up (-down) component is defined by the unit vector $\mathbf{n}_{\uparrow(\downarrow)} = (p_x, p_y, h_{z;\uparrow(\downarrow),\mathbf{k}})/E$. Since $f(\mathbf{k}) = 0$ at $(\pi, 0)$, $\mathbf{n}_{\uparrow,\downarrow} = \mathbf{n}$ at this Dirac point. Near the Dirac point $(0,0)$, $\mathbf{n}_{\uparrow,\downarrow} = (-2tq_y, 2tq_x, -M - 4t' \mp 4\Delta)/E$. For $M < 4t'$, the energy gap at $(0,0)$ closes at $\Delta = \Delta_0 = \frac{1}{4}(M + 4t')$. When $\Delta > \Delta_0$, $\mathbf{n}_\downarrow$ at $(0,0)$ changes from the right frame to the left frame while $\mathbf{n}_\uparrow$ remains in the right frame. Therefore, $C_\uparrow = 1$ while the pseudospin-down component becomes topological trivial with $C_\downarrow = 0$. This can also be seen from the effective chemical potential of the components; only $\mu_{\uparrow,(0,0)} = -h_{z,\uparrow;(0,0)} > 0$ satisfies the weak pairing condition, while the other three are in the strong pairing regime, i.e. $\mu_{\downarrow;(0,0)} = -h_{z,\downarrow;(0,0)} < 0$ and $\mu_{\uparrow,\downarrow;(\pi,0)} = -h_{z,\uparrow,\downarrow;(\pi,0)} < 0$. Thus, the ground state wave function is given by $\Psi(\{\mathbf{r}^a_i, \mathbf{r}^b_i\}) \sim \mathrm{Pf}[g_\uparrow(\mathbf{r}_i - \mathbf{r}_j)]$, which is identical to the charge neutral Moore-Read Pfaffian in the long wavelength limit. The ground state is three-fold degenerate[28]. A pair of vortices are the same as the Moore-Read non-abelian anyons[22]

$$\Psi_v(\eta_1, \eta_2) \sim \mathrm{Pf}\{[(z_i - \eta_1)(z_j - \eta_2) + (1 \leftrightarrow 2)]g_\uparrow(\mathbf{r}_i - \mathbf{r}_j)\}.$$

However, each vortex again carries charge $e/2$. The safe distance between the vortices is also determined by the band gap.

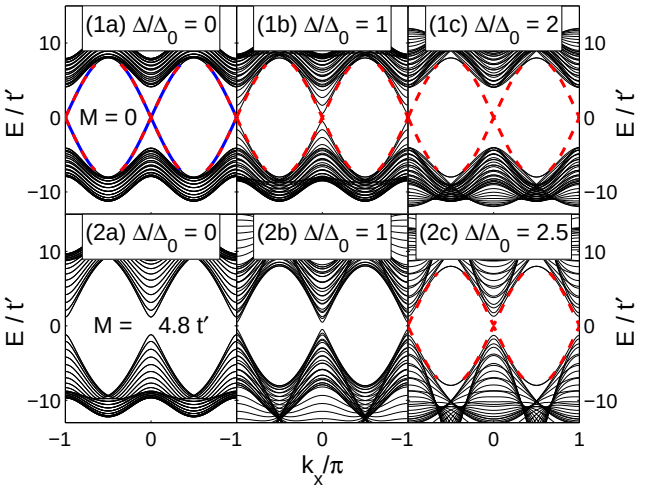

FIG. 3: (color online) The energy dispersion E along k_x showing the evolution of the edge states with proximity induced pairing Δ. Top panel starts with (1a) the QAHE state ($M < 4t'$) while the bottom panel starts with (1b) the insulating state ($M > 4t'$) when $\Delta = 0$. The gap closes at $\Delta = \Delta_0$ (1b and 2b). The chiral edge states located at the $y = 0$ and $y = L$ boundaries are marked by red dashed lines and, in the case of degeneracy, the blue solid lines. $t = 4t'$.

C. Insulator-QAHE transition and non-abelian anyons

Interestingly, for $M > 4t'$, the model H_0 with the proximity effect is topologically trivial with $C_{\uparrow,\downarrow} = 0$, since the poles at $(\pi, 0)$ and $(0, 0)$ are in the opposite frames (See Fig. 2(b)). In this case $v_s \sim 1$, but $u_s \sim q_y - iq_x$ near $(0,0)$ while $u_s \sim q_y + iq_x$ near $(\pi, 0)$. As a result, the quasiparticle local wave functions near the Dirac points are the holomorphic $(1, 1, -1)$-state for $(0, 0)$ and the anti-holomorphic $(1, 1, -1)$-state for $(\pi, 0)$. They contribute to the Hall conductance with the same magnitude but opposite signs and lead to an insulating state.

In the presence of proximity induced pairing, the insulating gap closes at $\Delta = \Delta_0$. When $\Delta > \Delta_0$, the pseudospin-up component is pushed into the strong pairing regime near (0,0), i.e. $\mu_{\uparrow,(0,0)} < 0$, while all others remain unchanged. Thus the low energy physics is dominated by the Pfaffian of the up-spin component near $(\pi, 0)$ with winding numbers $C_\uparrow = -1$ and $C_\downarrow = 0$. This is therefore a transition from an insulator to a non-abelian QAHE state with Hall conductance $-e^2/h$ where vortex excitations are non-abelian anyons[29].

IV. EDGE STATES AND MAJORANA FERMION MODES

Next, we present explicit calculations of the edge state spectrum of the total Hamiltonian H under an open boundary condition along the y-direction of a strip. The

existence of the nontrivial topological invariants implies stable gapless edge modes separated from the gapped bulk excitations. For a small $M < 4t'$, say $M = 0$, gapless chiral edge states appear across $k_x = 0$ as shown in Fig. 3. There are indeed two degenerate chiral edge states in this $(1, 1, -1)$ abelian QAHE state (Fig. 3(1a)). The gap closing is demonstrated in Fig. 3(1b). After the proximity induced topological phase transition, a single edge mode survives (Fig. 3(1c)) in the non-abelian QAHE state. The lower panel of Fig. 3 starts with the non-topological insulator at $M = 4.8t'$ where edge states are absent. The proximity effect causes the topological gap closing transition (Fig. 3(2b)) and the emergence of a single edge state in non-abelian QAHE state (Fig. 3(2c)).

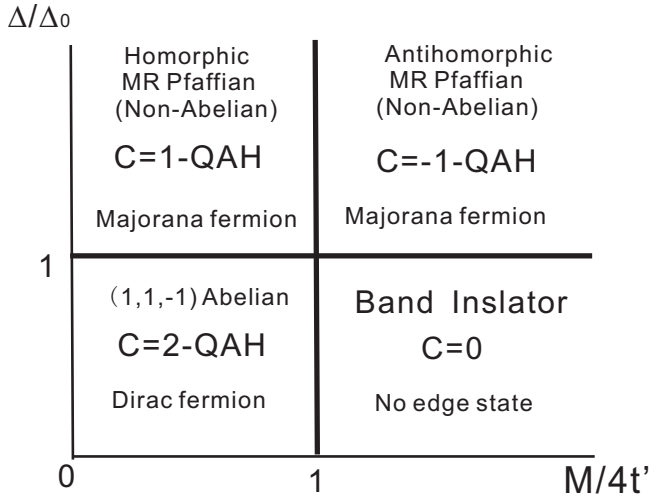

FIG. 4: The phase diagram with the Chern numbers, the ground state wave functions and the gapless edge modes.

These numerical calculations confirm the analysis and results obtained in previous sections. For $k_x = 0 + q_x \ll 1$, the gapless edge modes can be written as $\psi_s(0; q_x) = u_s(0; q_x)c_{s,0;q_x} + v_s(0; q_x)c^\dagger_{s,0;-q_x}$. At $q_x = 0$, we have $u_s(q_x) = v(q_x) = \frac{1}{\sqrt{2}}$ and $\psi^\dagger_s(0; 0) = \psi_s(0; 0)$. These are indeed the Majorana fermion zero modes. In the (1,1,-1)-state, both $\psi_{\uparrow,\downarrow}$ exist and combine into a complex neutral Dirac fermion, which is consistent with the neutrality of the bulk ground state in the long wavelength limit. For both the holomorphic Moore-Read Pfaffian (Fig. 3(1c)) and the anti-holomorphic Pfaffian states (Fig. 3(2c)) induced by the proximity effect, there is only one Majorana mode on the edge, consistent with the existence of the non-abelian anyons.

V. PHASE DIAGRAM AND CONCLUSIONS

In Fig. 4, we summarize our results in a schematic phase diagram for this class of two-component abelian and nonabelian QAHE. While the interesting non-abelian phase was confirmed after a superconductor proximity, the $\mathcal{C} \cdot \mathcal{S}$ discrete symmetry leads to a new topological order with abelian anyon even without a superconductor proximity and no interaction between electrons are concerned. Finally, we argued that the partial particle-hole transformation may be a general duality between a topological insulator and a topological superconductor.

ACKNOWLEDGEMENTS

We thank Dung-Hai Lee for useful discussions. This work was supported by National Natural Science Foundation of China, the national program for basic research of MOST of China (YY,XX), the Key Lab of Frontiers in Theoretical Physics of CAS(YY), in part by DOE DE-FG02-99ER45747 and NSF DMR-0704545 (ZW), and DOE DE-FG02-04ER46124(XL,XX).

* Correspondences send to yyu@itp.ac.cn

[1] K. von Klitzing, G. Dorda, and M. Pepper, Phys. Rev. Lett. **45**, 494(1980).
[2] D. J. Thouless, M. Kohmoto, M.P. Nightingale, and M. den Nijs, Phys. Rev. Lett. **49**, 405 (1982).
[3] F. D. M. Haldane, Phys. Rev. Lett. **61**, 2015(1988).
[4] For rewiev, see M. Z. Hasan and C. L. Kane, Rev. Mod. Phys. **82**, 3045 (2010) ; X. L. Qi and S. C. Zhang, arXiv: 1008.2026 (2010).
[5] C. L. Kane and E. J. Mele, Phys. Rev. Lett. **95**, 146802 (2005).
[6] C. L. Kane and E. J. Mele, Phys. Rev. Lett. **95**, 226801 (2005).
[7] B. A. Bernevig, T. L. Hughes, and S. C. Zhang, Science **314**, 1757 (2006).
[8] M. König, S. Wiedmann, C. Brüne, A. Roth, H. Buhmann, L. Molenkamp, X. L. Qi and S. C. Zhang, Science **318**, 766 (2007).
[9] J. E. Moore and L. Balents, Phys. Rev. B **75**, 121306 (2007).
[10] L. Fu, C. L. Kane, and E. J. Mele , Phys. Rev. Lett. **98**, 106803 (2007).
[11] R. Roy, Phys. Rev. B **79**, 195322 (2009).
[12] L. Fu, and C. L. Kane, Phys. Rev. B **76**, 045302 (2007).
[13] D. Hsieh, D. Qian, L. Wray, Y. Xia, Y. S. Hor , R. J. Cava and M. Z. Hasan, Nature **452**, 970 (2008).
[14] X. L. Qi, Y. S. Wu, and S. C. Zhang, Phys. Rev. B **74** , 085308 (2006).
[15] C. X. Liu, X.-L. Qi, X. Dai, Z. Fang, and S.-C. Zhang, Phys. Rev. Lett. **101**, 146802 (2008).
[16] R. Yu, W. Zhang, H. J. Zhang, S. C. Zhang, X. Dai, and Z. Fang , Science **329**, 61 (2010).
[17] Y. Zhang and C. Zhang, arXiv:1009.1200.
[18] Z. Qiao, S. A. Yang, W. Feng, W.-K. Tse, J. Ding, Y. Yao, J. Wang and Q. Niu, Phys. Rev. B **82**, 161414 (2010).
[19] L. B. Shao, S.-L. Zhu, L. Sheng, D. Y. Xing, and Z. D. Wang, Phys. Rev. Lett. **101**, 246810 (2008).
[20] X. J. Liu, X. Liu, C. Wu, and J. Sinova , Phys. Rev. A **81**, 033622 (2010).
[21] M. Zhang, H.-H. Hung, C. Zhang, and C. Wu, arXiv:1009.2133.
[22] G. Moore and N. Read, Nucl. Phys. B **360**, 362 (1991).
[23] A. Y. Kitaev, Ann. Phys. (N.Y.) **303**, 2 (2003).
[24] L. Fu and C. L. Kane, Phys. Rev. Lett. **100**, 096407 (2008).
[25] J. D. Sau, R. M. Lutchyn, S. Tewari, and S. Das Sarma, Phys. Rev. Lett. **104**, 040502 (2010).
[26] B. I. Halperin, Helv. Phys. Acta **56**, 783 (1983); Surf. Sci. **305**, 1 (1994).
[27] T. L. Ho, Phys. Rev. Lett. **75**, 1186 (1995).
[28] N. Read and D. Green, Phys. Rev. B **61**, 10267 (2000).
[29] X. L. Qi, T. L. Hughes, and S. C. Zhang, Phys. Rev. B **82**, 184516 (2010).